Differences in atrial fibrillation-associated proteins between the left and right atrial appendages from patients with rheumatic mitral valve disease: A comparative proteomic analysis

HAI LIU[1,2*], GUANGXIAN CHEN[1*], HONGSHENG ZHENG[3*], HAN QIN[1], MENGYA LIANG[1], KANGNI FENG[1] and ZHONGKAI WU[1]

[1]Second Department of Cardiac Surgery, First Affiliated Hospital of Sun Yat-Sen University, Guangzhou, Guangdong 510080; [2]Third Department of Cardiac Surgery, First Affiliated Hospital of Zhengzhou University, Zhengzhou, Henan 450052; [3]Department of Cardiac Surgery, Henan Provincial Chest Hospital, Zhengzhou, Henan 450008, P.R. China

Received August 26, 2015; Accepted September 15, 2016

DOI:10.3892/mmr.2016.5776

Abstract. The majority of proteomic studies have focused on identifying atrial fibrillation (AF)-associated proteins in the right atrium (RA), thus potential differences in AF-associated proteins between the RA and left atrium (LA) remain unknown. The aim of the present study was to perform proteomic analysis to compare the potential differences in AF-associated proteins between the right atrial appendage (RAA) and left atrial appendage (LAA) in patients with rheumatic mitral valve disease (RMVD). RAA and LAA tissues were obtained from 18 patients with RMVD (10 with AF) during mitral valve replacement surgery. Two-dimensional fluorescence difference gel electrophoresis (2-D DIGE) proteomics analysis was performed using these tissues to identify AF-associated proteins in RAA and LAA. Subsequently, the proteomics data was validated using western blot analysis of nine selected proteins. In RAA, 32 AF-associated proteins were significantly dysregulated (15 upregulated and 17 downregulated). In LAA, 31 AF-associated proteins were significantly dysregulated (13 upregulated and 18 downregulated). Among these AF-associated proteins, 17 were AF-associated in both RAA and LAA, 15 were AF-associated only in RAA, and 14 were AF-associated only in LAA. Amongst the differentially expressed proteins, western blot analysis validated the results for 6 AF-associated proteins, and demonstrated similar distributions in RAA and LAA compared with the 2-D DIGE results. Of these proteins, 2 proteins were AF-associated in both RAA and LAA, 2 were AF-associated only in RAA, and 2 were AF-associated only in LAA. Additionally, the different distributions of AF-associated proteins in the RAA and LAA of patients with RMVD was analyzed, which may reflect the different regulatory mechanisms of the RA and LA in AF. These findings may provide new insights into the underlying molecular mechanisms of AF in patients with RMVD.

Correspondence to: Dr Zhongkai Wu, Second Department of Cardiac Surgery, First Affiliated Hospital of Sun Yat-Sen University, 58 Zhongshan II Road, Guangzhou, Guangdong 510080, P.R. China
E-mail: wuzhk@mail.sysu.edu.cn

Abbreviations: AF, atrial fibrillation; SR, sinus rhythm; RMVD, rheumatic mitral valve disease; RA, right atrium; LA, left atrium; RAA, right atrial appendage; LAA, left atrial appendage; 2-D DIGE, two-dimensional fluorescence difference gel electrophoresis; IEF, isoelectric focusing; MALDI-TOF/TOF MS, matrix-assisted laser desorption/ionization time-of-flight mass spectrometer/mass spectrometry; MS/MS, mass spectrometer/mass spectrometry; PMF, peptide mass fingerprint

[*]Contributed equally

Key words: atrial fibrillation, rheumatic mitral valve disease, right atrial appendage, left atrial appendage, proteomics

Introduction

Atrial fibrillation (AF) is the most common sustained arrhythmia in clinical practice (1). It often occurs concomitantly with other cardiovascular diseases, including hypertension, congestive heart failure, coronary artery disease, and valvular heart disease (2,3). Rheumatic mitral valve disease (RMVD), a major cardiovascular disease in developing countries affected by rheumatic fever, is a major clinical risk factor for AF (4,5). Development of effective therapies and preventative strategies are crucial for the control of AF-associated morbidity and mortality. However, Currently, medical interventions for AF are relatively limited, as the precise mechanisms of AF have not been completely elucidated. Therefore, novel methods to probe the underlying mechanisms of AF and potential novel mechanism-based therapeutic strategies are required (6).

The field of cardiovascular proteomics has shed new light on understanding the regulatory mechanisms of AF (7). Progression from paroxysmal AF to persistent, and then to permanent AF involves complex changes in gene expression, and subsequent changes in protein expression and activity (8). Proteomic techniques are a powerful tool to evaluate global protein changes in diseased hearts and discover novel proteins, diagnostic biomarkers, and potential drug targets for the

development of novel therapeutic agents (7). Two-dimensional fluorescence difference gel electrophoresis (2-D DIGE) can provide an overview of the proteome during disease (9). Previous use of proteomic methods have identified differentially expressed proteins associated with AF (AF-associated proteins) in several animal models (10,11) and human heart tissue (12-16).

Genomic (8,17), morphological (18,19), and electrophysiological (20-22) differences have been observed between the right atrium (RA) and left atrium (LA). This suggests that different mechanisms regulate the RA and LA in AF (23). Thus, it is unsurprising that the AF-associated proteins of the RA may differ from those of the LA. However, the majority AF proteomics studies have primarily focused on the RA. Thus, potential differences in AF-associated proteins between RA and LA remain unknown. Given the complexity of AF progression, a better understanding of the differences in AF-associated proteins between RA and LA may elucidate novel cardioprotective strategies.

Thus, the aim of the present study was to perform 2-D DIGE proteomics analysis to compare potential differences of AF-associated proteins in the right atrial appendage (RAA) and left atrial appendage (LAA) from patients with RMVD that were either in sinus rhythm (SR) or AF.

Materials and methods

Ethics approval. Approval for this study was obtained from the Human Ethics Committee at the First Affiliated Hospital of Sun Yat-Sen University. The investigation complied with the principles that govern the use of human tissues outlined in the Declaration of Helsinki. All patients provided informed consent prior to participation in the study.

Human tissue preparation. Human tissue preparation was performed as previously described (8). Briefly, RAA and LAA tissues were obtained from the same patient as surgical biopsies at the time of the mitral valve replacement surgery (RAA from cannulation site and LAA during ligation). Tissues were immediately snap frozen in liquid nitrogen, and stored at -80˚C prior to use. Tissue samples from the RAA and LAA were obtained from 18 patients with RMVD. The patients in the SR group (n=8) had no history of AF. The patients in the AF group (n=10) presented with a documented history of arrhythmias for >6 months prior to surgery. The diagnosis of AF was reached by evaluating medical records and 12-lead electrocardiogram findings. Patients with SR also had no history of using antiarrhythmic drugs and were screened to ensure that they had never experienced AF. Routine pre-operative color Doppler echocardiography was performed on all patients. Pre-operative functional status was recorded according to New York Heart Association (NYHA) classifications.

Preparation of protein extracts. Protein extracts were isolated from tissues based on previously published protocols (24). Briefly, tissues (approximately 0.1 g) were homogenized in lysis buffer [7 M urea, 2 M thiourea, 30 mM Tris, 4% (w/v) CHAPS cell lysis buffer, 40 mM dithiothreitol (DTT), 0.6 mM phenylmethylsulfonyl fluoride] and the supernatant was collected following centrifugation (2,000 x *g*, 4˚C, 40 min). To remove non-protein material from the extract and determine the final protein concentration, the 2-D Clean-up kit (GE Healthcare Life Sciences, Chalfont, UK) and 2-D Quant kit (GE Healthcare Life Sciences) were used according to manufacturer's instructions.

Protein labeling with CyDye DIGE fluorophores. Protein extracts were labeled with three CyDye DIGE fluorophores, Cy2, Cy3 and Cy5 (GE Healthcare Life Sciences), for 2-D DIGE technology, according to the manufacturer's protocols. Briefly, equal amounts of protein from the same group were pooled and divided into four equal portions (50 μg each). The latter portions were labeled with 400 pmol Cy3 or Cy5 according to the experimental design. A pooled sample consisting of equal amounts of all samples was used as the pooled internal standard and labeled with Cy2. After incubating samples on ice for 30 min in the dark, the labeling reaction was stopped with 10 mM lysine. For each gel, Cy2-, Cy3- and Cy5-labeled proteins (50 μg each) were mixed and calibrated to 450 μl with rehydration buffer [7 M urea, 2 M thiourea, 4% (w/v) CHAPS cell lysis buffer, 40 mM DTT, 1% IPG buffer (pH 4-7), 0.002% (w/v) bromophenol blue].

2-D electrophoresis. 2-D electrophoresis was performed as previously described (25). The labeled protein mixture in each gel was applied to ImmobilineDryStrip strips (24 cm, pH 4-7; GE Healthcare Life Sciences). Isoelectric focusing (IEF) was performed with an EttanIPGphor II apparatus (GE Healthcare Life Sciences) using the follow steps: 30 V for 12 h, 500 V for 1 h, 1,000 V for 1 h, and 10,000 V for up to a total of 85,000 V/h. Following IEF, the proteins were reduced and alkylated by successive 15 min treatments with equilibration buffer containing 2% (w/v) DTT followed by 2.5% (w/v) iodoacetamide. Proteins were then resolved on 12.5% SDS-PAGE gels using an EttanDALTsix instrument (GE Healthcare Life Sciences). In order to facilitate mass spectrometry analysis, 500 μg of unlabeled pool protein sample was run in parallel on a preparative gel and stained by Deep Purple staining (GE Healthcare Life Sciences) according to the manufacturer's instructions.

Gel image acquisition and analysis. Gel images were acquired on a Typhoon 9400 scanner (GE Healthcare Life Sciences) and analyzed using DeCyder software (version 6.0; GE Healthcare Life Sciences) as previously described (26,27). Briefly, Cy2-, Cy3- and Cy5-labeled images of each gel were scanned with excitation/emission wavelengths of 488/520, 532/580 and 633/670 nm, respectively. Following CyDye labeling, signals were imaged and the gels were stained using Deep Purple total protein stain (GE Healthcare Life Sciences) according to standard protocols and scanned with excitation/emission wavelengths of 532/560 nm. The 2-D DIGE gel images were subsequently analyzed with DeCyder software. Protein expression patterns for SR-RAA were compared with AF-RAA, and SR-LAA were compared with AF-LAA. Ratios of proteins that increased or decreased >1.5-fold (*t*-test, $P<0.05$) were considered significant changes (9). The corresponding protein spots were also selected in the stained preparative gel for spot picking.

Spot picking and enzymatic digestion. Selected protein spots in the preparative gels were automatically picked and handled in an Ettan Spot Handling Workstation (GE Healthcare Life Sciences) for the preparation of the protein sample for matrix-assisted laser desorption/ionization time-of-flight mass spectrometer/mass spectrometry (MALDI-TOF/TOF MS) analysis. In the automated procedure, the selected protein spots were picked, washed with 15 mM NH_4HCO_3 and 50% v/v methanol, then digested with 20 ng/ml trypsin (sequencing grade; Promega Corporation, Madison, WI, USA) in 20 mM NH_4HCO_3 for 2 h at 37˚C. Tryptic peptides were extracted with 50% v/v acetonitrile (ACN) and 0.5% v/v trifluoroacetic acid (TFA), and dissolved in 5 mg/ml R-cyano-4-hydroxycinnamic acid (GE Healthcare Life Sciences) matrix in 50% (v/v) ACN and 0.1% (v/v) TFA. Finally, samples were spotted on the mass spectrometry sample plate.

MALDI-TOF/TOF MS analysis and database searching. Mass spectrometry analysis was performed using an Utraflex III MALDI-TOF/TOF MS (Bruker Corporation, Ettlingen, Germany) operating in a positive ion reflector mode. Monoisotopic peak masses were acquired in a mass range of 700-4,000 Da, with a signal-to-noise ratio >200. Four of the most intense ion signals, excluding common trypsin autolysis peaks and matrix ion signals, were automatically selected as precursors for mass spectrometer/mass spectrometry (MS/MS) acquisition. Peptide mass fingerprint (PMF) combined with MS/MS spectra was blasted against the NCBInr database using the Biotools software (version 3.2; Bruker Corporation) and MASCOT version 2.2 (Matrix Science, Inc., Boston, MA, USA). Search parameters were set as follows: *Homo sapiens*, trypsin cleavage, one missed cleavage allowed, carbamidomethylation as fixed modification, oxidation of methionines allowed as variable modification, peptide mass tolerance at 50 ppm, and fragment tolerance at 0.5 Da. The criteria for successfully identifying a protein was as follows: Ion score confidence interval (%) for PMF and MS/MS data >95%, peptide count (hit) ≥4, and at least two peptides of distinct sequence were identified in MS/MS analysis.

Protein categorization and protein-protein interaction prediction. Protein categorization and protein-protein interaction predictions were performed as previously described (9). Briefly, the identified proteins were classified, according to the Protein Analysis Through Evolutionary Relationships (PANTHER) system (http://www.pantherdb.org), which classified genes and proteins by their function. The PANTHER ontology, a highly controlled vocabulary (ontology terms) by molecular function, biological processes and molecular pathways, was employed to categorize proteins into families and subfamilies with shared function. The prediction of protein-protein interactions was performed by utilizing the Search Tool for the Retrieval of Interacting Genes/Proteins (STRING) system (http://www.string-db.org). STRING is a database of known and predicted protein interactions that include direct (physical) and indirect (functional) associations.

Western blot analysis. Western blot analysis was performed as previously described (28). Briefly, protein lysates were prepared from human tissues, separated on SDS-PAGE, transferred to a polyvinylidene difluoride membrane, and subjected to immunoblotting at 4˚C overnight with the following antibodies: Anti-aldo-keto reductase family 1 member B10 (AKR1B10; diluted 1:10,000; polyclonal antibody; cat. no. S1646; Epitomics, Burlingame, CA, USA), anti-crystallin α B (CRYAB; diluted 1:2000; polyclonal antibody; cat. no. PAB7394; Abnova Corporation, Taipei, Taiwan), anti-annexin 4 (ANAX4; diluted 1:800; polyclonal antibody; cat. no. H00000307-B01P; Abnova Corporation), anti-G protein subunit α o1 (GNAO1; diluted 1:10,000; polyclonal antibody; cat. no. S3107; Epitomics), anti-ribonuclease H1 (RNase H1; diluted 1:800; monoclonal antibody; cat. no. ab56560; Abcam, Cambridge, MA, USA), anti-moesin (MSN; diluted 1:2,000; polyclonal antibody; cat. no. PAB7062; Abnova Corporation), anti-nestin (NES; diluted 1:6,000; polyclonal antibody; cat. no. PAB12375; Abnova Corporation) and anti-transferrin (diluted 1:8,000; polyclonal antibody; cat. no. S0860; Epitomics), anti-osteoglycin (diluted 1:500; monoclonal antibody; cat. no. 5518-1; Epitomics). β-actin was assessed as a loading control (diluted 1:20,000; monoclonal antibody; cat. no. 60008-1-Ig; ProteinTech Group, Inc., Chicago, IL, USA). After washing, membranes were incubated with horseradish peroxidase (HRP)-conjugated secondary antibodies (goat anti-mouse, cat. no. SA00001-1; goat anti-rabbit, cat. no. SA00001-2; or rabbit anti-goat, cat. no. SA00001-4; all from ProteinTech Group, Inc.) and visualized using an enhanced chemiluminescence western blot detection system (Immobilon Western Chemiluminescent HRP substrate; Merck Millipore, Darmstadt, Germany) on X-ray film (Kodak, Rochester, NY, USA). All the proteins were detected on the same blot. For certain protein with molecular weights very close to each other, the blots were stripped and reprobed using Restore™ PLUS Western Blot Stripping Buffer(Thermo Fisher Scientific Inc., Waltham, MA, USA) according to the manufacturer's instructions. Images were scanned and analyzed using Kodak Molecular Imaging software (version 5.0). Non-specific binding was subtracted, and the band signals were expressed as relative protein amounts compared with β-actin protein levels.

Statistical analysis. Data of clinical characteristics of patients and western blot quantification are presented as the

Table I. Clinical characteristics of the patients with SR and AF.

Characteristic	SR (n=8)	AF (n=10)
Gender (male/female)	5/3	5/5
Age (years)	50.16±6.88	51.42±7.12
LA size (mm)	43.31±3.23	57.65±5.08[a]
LVEDD (mm)	48.35±5.15	50.13±3.07
LVEF (%)	61.34±5.66	58.71±3.81
NYHA class		
II	6	7
III	2	3

[a]P<0.05 vs. SR patients. Values are presented as the mean ± standard deviation. SR, sinus rhythm; AF, atrial fibrillation; LA, left atrium; LVEDD, left ventricular end-diastolic diameter; LVEF, left ventricular ejection fraction; NYHA class, New York Heart Association classifications.

Table II. Differential proteins identified by mass spectrometry following 2-D DIGE of the RAA and LAA samples.

Accession no.[a]	MW (kDa)	pI	Av. ratio[b]		*t*-test		Protein name
			RAA[c]	LAA[d]	RAA[c]	LAA[d]	
In RAA and LAA (n=17)							
gil88699	2.4	11.55	1.7	2.36	0.0065	0.013	T-cell receptor β chain J region (clone HBP22)-human (fragment)
gil7669550	124	5.5	1.56	1.5	0.0012	0.0044	Vinculin isoform meta-VCL
gil5669804	72	9.1	-1.76	-1.83	0.016	0.00039	Polycystin-2-like protein
gil42543698	42	6.62	1.57	1.5	0.038	0.011	Chain A, The Crystal Structure Of The Human Hsp70 Atpase Domain
gil41350923	110	5.85	1.61	2.06	0.011	0.0017	Collagen, type VI, α 2
gil386973	61	5.3	-1.88	-1.87	0.022	0.00066	β-Myosin heavy chain
gil386972	62	5.3	-1.88	-1.91	0.01	0.0019	α-Myosin heavy chain
gil386970	71	5.32	-1.79	-1.94	0.019	0.00019	Myosin heavy chain β-subunit
gil33150528[e]	34	5.33	-1.75	-2.01	0.012	0.0079	Osteoglycin
gil223468663[e]	36	7.67	-1.68	-2.02	0.026	0.0026	Aldo-ketoreductase family 1 member B10
gil19908424	54	5.21	1.99	1.94	0.036	0.038	Mutant desmin
gil189617[e]	36	5.65	1.55	1.73	0.021	0.026	Protein PP4-X
gil119622366	8.0	10.91	-2.23	-2.08	0.018	0.00011	hCG1813095
gil119622046	16	12.02	-1.58	-1.68	0.0019	0.023	hCG1646228
gil119612724	30	4.88	-1.79	-2.02	0.014	0.0028	Actin, α, cardiac muscle, isoform CRA_c
gil119586559	224	5.58	-2.57	-2.14	0.0082	0.0052	Myosin, heavy polypeptide 6, cardiac muscle, α (cardiomyopathy, hypertrophic 1), isoform CRA_b
gil119576987	34	9.33	-1.88	-2.03	0.011	0.0041	DNA cross-link repair 1B
Only in RAA (n=15)							
gil94981553	19	4.92	-2.72	-	0.024	-	Myosin regulatory light chain 2, ventricular/cardiac muscle isoform
gil62897129	71	5.28	-1.55	-	0.027	-	Heat shock 70kDa protein 8 isoform 1 variant
gil55749932	54	5.21	2.04	-	0.0035	-	Desmin
gil51103391	12	8.98	-1.68	-	0.011	-	Immunoglobulin variable region VL kappa domain
gil5031875	65	6.4	1.6	-	0.017	-	Lamin-A/C isoform 2
gil46593007	53	5.94	4.82	-	0.048	-	Cytochrome b-c1 complex subunit 1, mitochondrial precursor
gil4505257[e]	68	6.08	1.62	-	0.029	-	Moesin
gil4505047	39	6.16	-1.63	-	0.023	-	Lumican precursor
gil4503057[e]	20	6.76	1.99	-	0.0016	-	α-Crystallin B chain
gil31615330	68	5.66	2.09	-	0.0091	-	Chain A, human serum albumin mutant R218h complexed with thyroxine
gil223170	47	5.54	1.56	-	0.032	-	Fibrinogen γ
gil145942333	9.6	5.5	1.79	-	0.019	-	Immunoglobulin heavy chain variable region
gil119581148	58	6.95	-1.69	-	0.002	-	Keratin 9
gil116283748[e]	66	5.15	-2.04	-	0.0068	-	Nestin protein
gil114615454	44	6.57	1.79	-	0.015	-	PREDICTED: dihydrolipoamide dehydrogenase isoform 1

Table II. Continued.

Accession no.[a]	MW (kDa)	pI	Av. ratio[b]		*t*-test		Protein name
			RAA[c]	LAA[d]	RAA[c]	LAA[d]	
Only in LAA (n=14)							
gil998467	3.1	4.41	-	1.57	-	0.044	48 kDa histamine receptor subunit peptide 4
gil62414289	54	5.06	-	2.71	-	0.0035	Vimentin
gil56204818	38	5.39	-	-1.84	-	0.0016	Actin, α 1, skeletal muscle
gil4885079	33	9.31	-	2.23	-	0.0085	ATP synthase subunit γ, mitochondrial isoform H (heart) precursor
gil48476973	137	5.29	-	-1.67	-	0.0047	Rhabdomyosarcoma antigen MU-RMS-40.7B
gil4501893	104	5.31	-	2.17	-	0.0078	α-Actinin-2
gil34811370	13	10.15	-	-2.26	-	0.0062	Chain B, crystal structure of the 46kDa domain of human cardiac troponin in the Ca^{2+} saturated form
gil34190601[e]	35	5.18	-	-1.69	-	0.00024	G protein subunit α o1 protein
gil22080672	9.6	10.96	-	1.6	-	0.00089	MHC class I antigen
gil15029922[e]	50	4.83	-	-1.67	-	0.011	Ribonuclease H1 protein
gil119618538	13	10.95	-	1.76	-	0.0086	hCG2016250, isoform CRA_g
gil119612436	36	8.27	-	-1.97	-	0.0002	hCG1779566, isoform CRA_a
gil110590599[e]	77	6.85	-	1.58	-	0.014	Chain A, apo-human serum transferrin
gil109102505	35	5.82	-	-1.6	-	0.0024	PREDICTED: similar to serine/threonine-protein phosphatase PP1-β catalytic subunit (PP-1B) isoform 1

[a]Accession number of NCBInr database. [b]Decreased or increased ratio of AF-RAA comparison with SR-RAA, and AF-LAA comparison with SR-LAA. [c]AF-RAA comparison to SR-RAA. [d]AF-LAA comparison with SR-LAA. [e]Selected for validation by western blotting. "-" indicates, not detected. AF, atrial fibrillation; SR, sinus rhythm; MW, molecular weight; RAA, right atrial appendage; LAA, left with appendage.

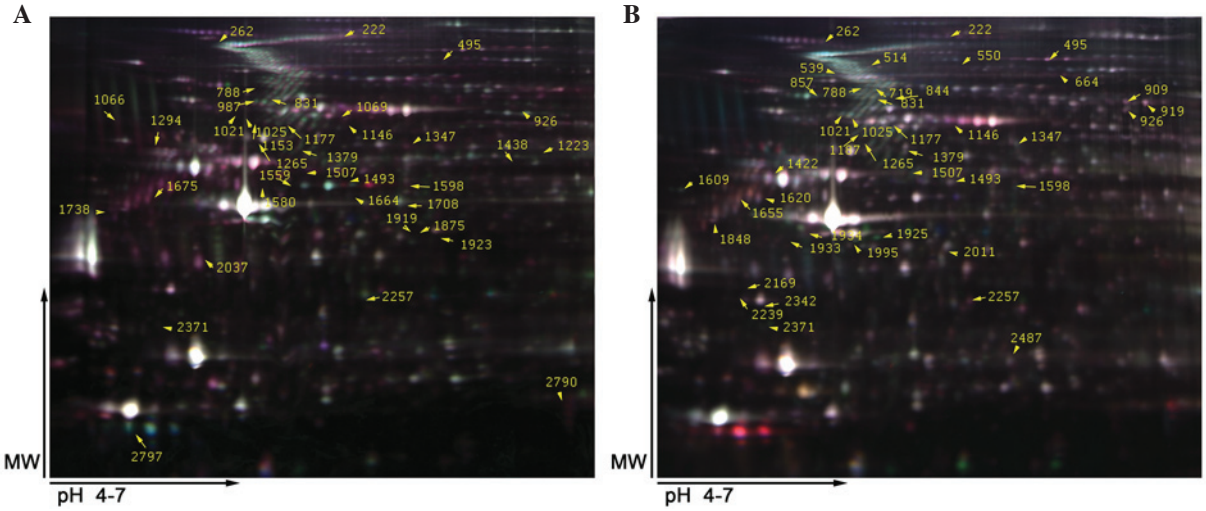

Figure 1. Analysis of RAA and LAA samples by 2-D DIGE analysis. Proteins extracted from AF (AF-RAA or AF-LAA) and SR (SR-RAA or SR-LAA) groups were labeled with Cy3 and Cy5, respectively. An internal standard comprised of proteins pooled from a combination of the AF-RAA, AF-LAA, SR-RAA and SR-LAA groups was labeled with Cy2 and included in all gels. The labeled AF and SR samples were mixed and separated on a 2-D DIGE gel (isoelectric focusing on pH 4-7 strips followed by 12.5% second dimension SDS-PAGE). Green spots represent downregulated proteins, and red spots represent upregulated proteins in AF samples compared with SR samples. The yellow arrows represent the identified proteins that exhibited significantly differential expression in the AF and SR samples. (A) AF-RAA vs. SR-RAA samples. (B) AF-LAA vs. SR-LAA samples. RAA, right atrial appendage; LAA, left atrial appendage; 2-D DIGE, two-dimensional fluorescence difference gel electrophoresis; AF, atrial fibrillation; SR, sinus rhythm; MW, molecular weight.

mean ± standard deviation. Student's *t*-test was used for statistical comparison of the data and to calculate significant differences in the relative abundance of individual protein spots between the two groups during 2-D DIGE analysis. The SPSS 16.0 software package (SPSS, Inc., Chicago, IL, USA) was used to conduct the statistical analyses and $P<0.05$ (two-tailed) was considered to indicate a statistically significant difference.

Results

Clinical characteristics of the patients with SR and AF. Tissue from RAA and LAA was obtained from each patient. No significant differences in terms of age, gender or NYHA class were observed between the SR and AF groups. Pre-operative color Doppler echocardiography demonstrated that the LA size of the patients with AF was significantly increased compared with the SR patients. However, no differences in the left ventricular end-diastolic diameter and left ventricular ejection fraction were observed between the groups (Table I).

2-D DIGE analysis and MALDI-TOF/TOF MS identification. Following 2-D DIGE analysis, a total of 2,813 spots were observed to be well matched across all gels using the DeCyder software analysis. The 2-D DIGE gel images are presented in Fig. 1. Following visual review, 61 protein spots of high abundance that exhibited significantly altered expression (AF-RAA vs. SR-RAA and AF-LAA vs. SR-LAA) were selected for MALDI-TOF/TOF MS analysis. A total of 32 differentially expressed proteins were identified, including 15 that were upregulated and 17 that were downregulated in the AF-RAA tissues compared with the SR-RAA tissues (Table II). Additionally, a total of 31 differentially expressed proteins, including 13 that were upregulated and 18 that were downregulated in the AF-LAA tissues compared with the SR-LAA tissues (Table II).

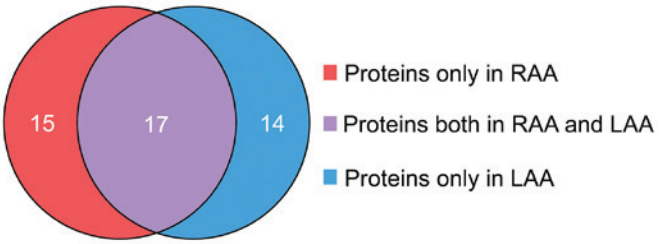

Figure 2. Distribution of differentially expressed proteins in RAA and LAA tissues. A total of 32 proteins were detected in RAA tissues and 31 proteins in LAA tissues. Additionally, 17 proteins were detected in both RAA and LAA tissues, and 15 proteins were detected only in RAA tissues and 14 proteins only in LAA tissues. RAA, right atrial appendage; LAA, left atrial appendage.

Comparison of differentially expressed proteins between RAA and LAA tissues. Using 2-D DIGE proteomics methodology, a total of 46 differentially expressed proteins were detected (in RAA or LAA tissues). Among these, 32 proteins were expressed in RAA tissues, and 31 proteins in LAA tissues. Furthermore, 17 proteins were identified in RAA and LAA tissues, whereas 15 proteins were detected only in RAA tissues and 14 proteins were only in LAA tissues (Table II; Fig. 2).

Classification of differentially expressed proteins and the protein-protein interaction network. According to cellular function and processes, a total of 46 differentially expressed proteins were distributed into categories based on molecular function, biological processes and protein classes using the PANTHER classification system. Results are presented in Fig. 3. The most dominant function that the identified proteins were involved in was structural activity (34.8%), followed by binding (19.6%), catalytic activity (19.6%), transporter activity (8.7%), receptor activity (8.7%), nucleic acid/protein binding

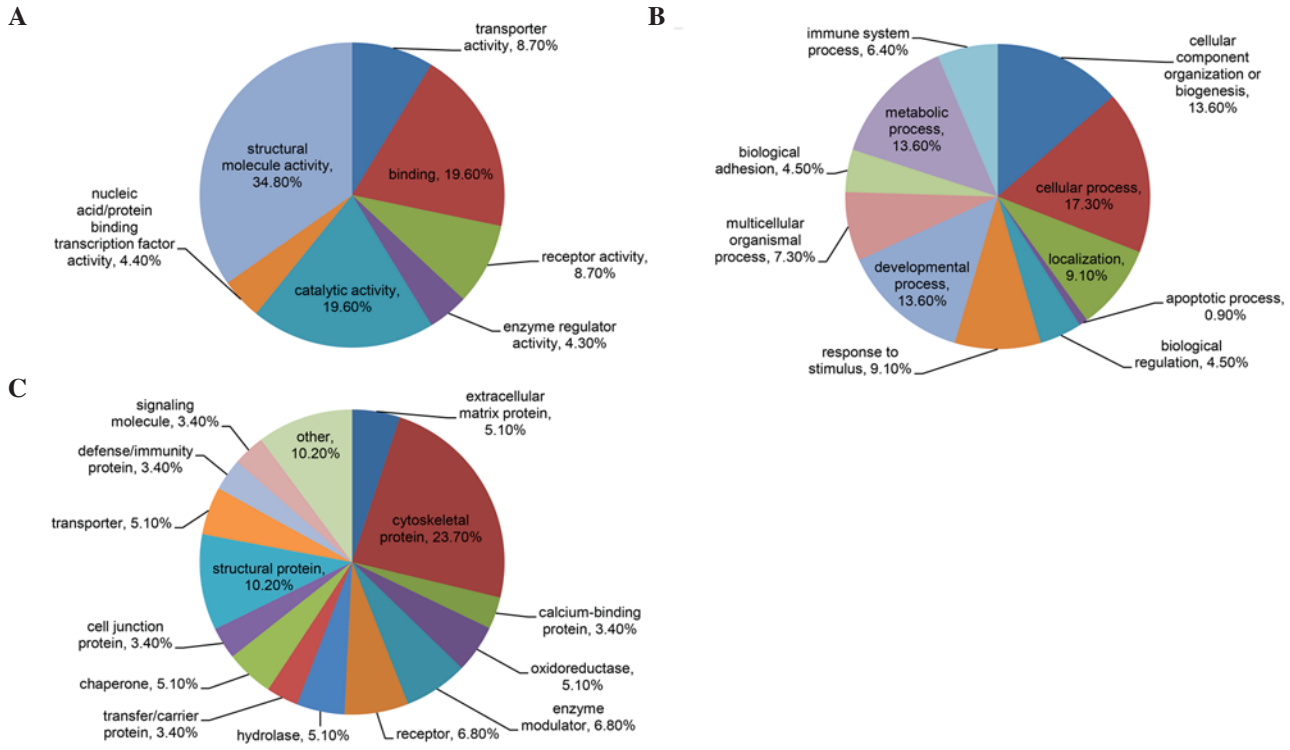

Figure 3. Classification of differentially expressed proteins using the PANTHER system. (A) Classification of the differentially expressed proteins according to molecular function. (B) Classification of the differentially expressed proteins according to biological processes. (C) Classification of the differentially expressed proteins according to protein class. PANTHER, Protein Analysis Through Evolutionary Relationships.

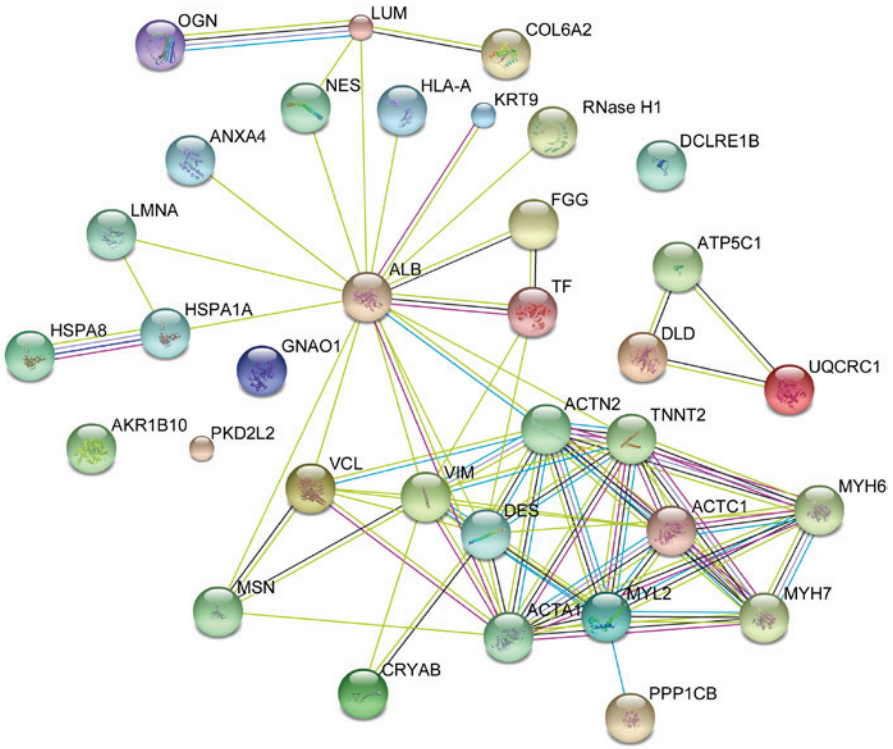

Figure 4. The protein-protein interaction network predicted by STRING. OGN, osteoglycin; LUM, lumican; COL6A2, collagen type VI α 2 chain; ANXA4, annexin A4; NES, nestin; HLA-A, major histocompatibility complex class I A; KRT9, keratin 9; RNase H1, ribonuclease H1; DCLRE1B, DNA cross-link repair 1B; LMNA, lamin A/C; ALB, albumin; FGG, fibrinogen γ chain; HSPA8, heat shock protein family A (Hsp70) member 8; HSPA1A, heat shock protein family A (Hsp70) member 1A; TF, transferrin; ATP5C1, ATP synthase H^+ transporting mitochondrial F1 complex γ polypeptide 1; DLD, dihydrolipoamide dehydrogenase; UQCRC1, ubiquinol-cytochrome c reductase core protein I; AKR1B10, aldo-keto reductase family 1 member B10; GNAO1, G protein subunit α o1; PKD2L2, polycystin 2 like 2 transient receptor potential cation channel; VCL, vinculin; VIM, vimentin; ACTN2, actinin α 2; TNNT2, troponin T2 cardiac type; DES, desmin; ACTC1, actin α cardiac muscle 1; MYH6, myosin heavy chain 6; MSN, moesin; ACTA1, actin α 1 skeletal muscle; MYL2, myosin light chain 2; MYH7, myosin heavy chain 7; CRYAB, crystallin α B; PPP1CB, protein phosphatase 1 catalytic subunit β; STRING, Search Tool for the Retrieval of Interacting Genes/Proteins.

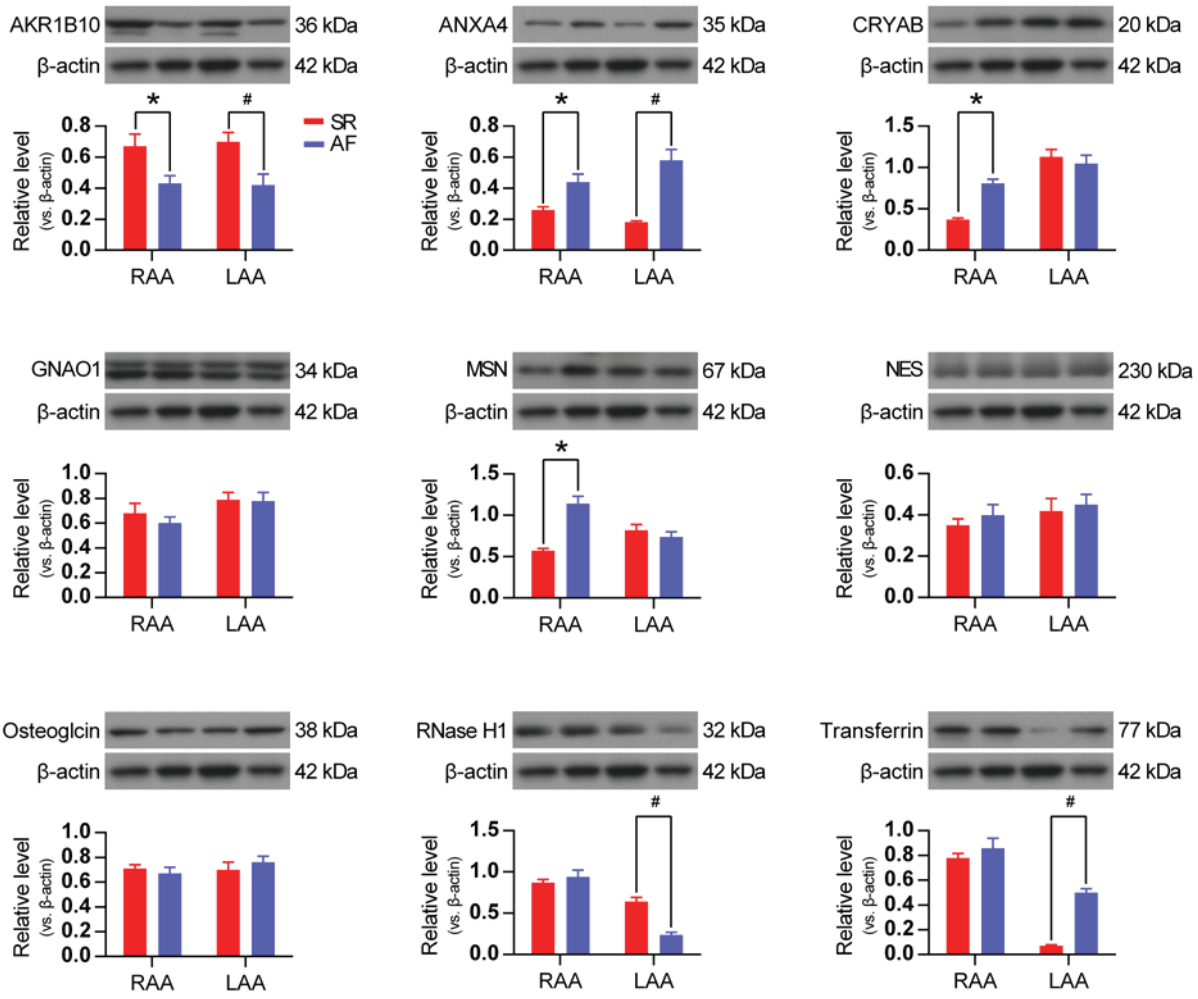

Figure 5. Validation of the two-dimensional fluorescence difference gel electrophoresis proteomics data by western blot analysis of nine selected differentially expressed proteins. β-actin is used as an internal loading control to normalize the results. Data are presented as the mean ± standard deviation of three independent experiments. *P<0.05, AF-RAA vs. SR-RAA. #P<0.05, AF-LAA vs. SR-LAA. AKR1B10, aldo-keto reductase family 1 member B10; ; SR, sinus rhythm; AF, atrial fibrillation; RAA, right atrial appendage; LAA, left atrial appendage; CRYAB, crystallin α B; GNAO1, G protein subunit α o1; MSN, moesin; NES, nestin; RNase H1, ribonuclease H1.

transcription factor activity (4.4%) and enzyme regulator activity (4.3%). The majority of the identified proteins had functions in cellular processes (17.3%), cellular component organization or biogenesis (13.6%), metabolic processes (13.6%) and developmental processes (13.6%). Other biological processes that the proteins were involved in included localization (9.1%), response to stimuli (9.1%), and multicellular organismal processes (7.3%). As for protein class, the majority of the proteins belonged in categories associated with cytoskeletal proteins (23.7%) and structural proteins (10.2%), while others belonged to categories associated with enzyme modulators (6.8%), receptors (6.8%) and calcium-binding proteins (3.4%).

The protein interaction network for the identified proteins was constructed by STRING (Fig. 4) in order to improve the understanding of the pathogenic mechanisms in AF with RMVD. Biological systems can be modeled as complex network systems with many interactions between components of different pathways. These interactions provide us with essential information about the function and behavior of the analyzed proteins (9).

Validation of the 2-D DIGE proteomics data by western blot analysis. To validate the data obtained from the 2-D DIGE proteomics, western blot analysis was performed on 9 selected proteins (Table II). According to the western blot data, AKR1B10 and ANAX4 were AF-associated proteins in RAA and LAA tissues (Fig. 5), whereas CRYAB and MSN were AF-associated proteins in only RAA tissues. RNase H1 and transferrin were AF-associated proteins only in LAA tissues (Fig. 5). The western blot data validated the results for all of these proteins, excluding osteoglycin, NES and GNAO1, AF-associated proteins which were not detected to be differentially expressed in the RAA or LAA of AF tissues when assessed using western blot analysis (Fig. 5).

Comparative analysis of the expression of six validated proteins between the RAA and LAA tissues from RMVD patients with SR. Six differentially expressed proteins were identified and validated using 2-D DIGE proteomics and western blot analysis. These proteins had different tissue distributions between RAA and LAA. Additionally, it was aimed to elucidate whether expression of these proteins was also different between RAA

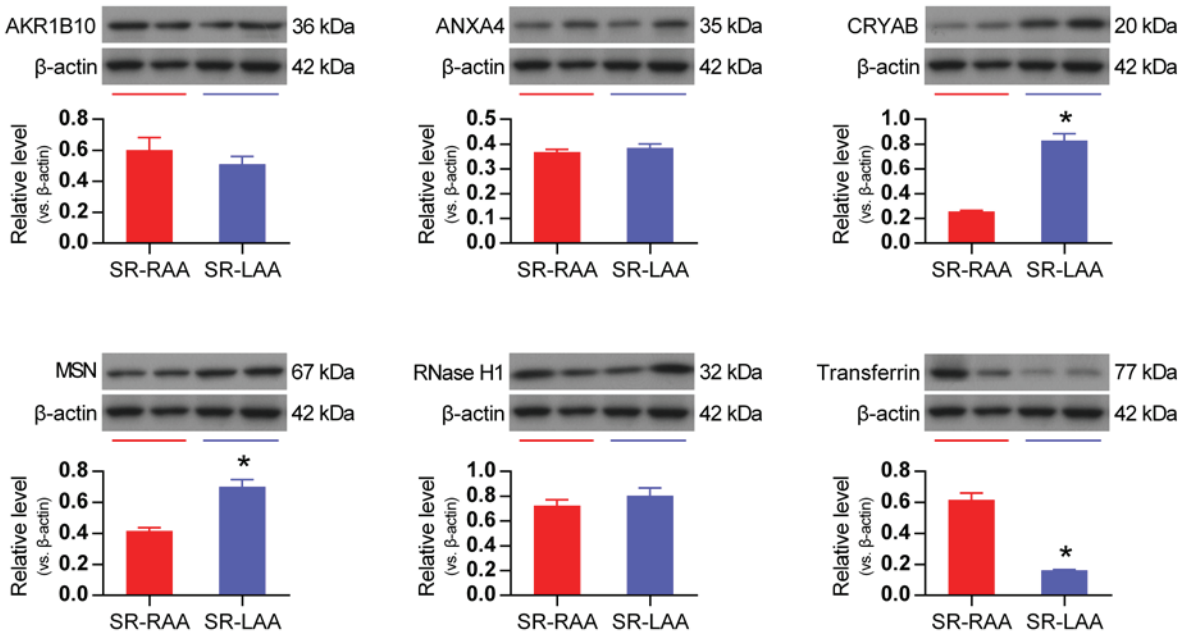

Figure 6. Comparison of the expression level of six validated AF-associated proteins in SR-RAA vs. SR-LAA by western blot analysis. β-actin is used as an internal loading control to normalize the results. Data are presented as the mean ± standard deviation of three independent experiments. *P<0.05 vs. SR-RAA. AKR1B10, aldo-keto reductase family 1 member B10; SR, sinus rhythm; RAA, right atrial appendage; LAA, left atrial appendage; CRYAB, crystallin α B; MSN, moesin; RNase H1, ribonuclease H1.

and LAA tissues based on SR status. Western blot analysis was used to compare the expression level of these proteins between the SR-RAA and SR-LAA groups. Expression levels of AKR1B10, ANAX4 and RNase H1 were not different in the RAA and LAA of patients with SR (Fig. 6). However, CRYAB and MSN expression was increased in the SR-LAA group compared with SR-RAA (Fig. 6). Transferrin expression was increased in the SR-RAA group compared with the SR-LAA group (Fig. 6).

Discussion

Previous studies have identified that both the RA (29,30) and LA (31,32) serve an important role in AF. However, intervention strategies that only target the RA or LA do not ameliorate all of the complications associated with AF (33-35). This may reflect the necessity to understand the different mechanisms involved in AF between the RA and LA. The development of AF involves complex changes in gene expression and subsequent changes in protein expression and activity. Thus, it is important to understand the protein mechanisms of AF to facilitate the development of potential novel mechanism-based therapeutic strategies. Proteomic technology provides a comprehensive strategy to investigate AF-associated proteins. Recently, there have been many proteomic studies associated with AF (10-16). However, the majority of proteomics studies on AF primarily focus on the RA and less on the LA. Although two previous studies (12,16) used proteomics analysis to identify AF-associated proteins in RA and LA tissue from patients with mitral valve disease, potential differences in AF-associated proteins between the RA and LA were not determined. Therefore, the potential differential expression of AF-associated proteins between the RA and LA remain unknown. To the best of our knowledge, the current study is the first to compare the potential differences of AF-associated proteins in the RA and LA from RMVD patients.

Profiling protein expression patterns at specific stages of disease can reflect the status of disease progression. We hypothesize that if there are different mechanisms involved in AF between the RA and LA, then changes in protein expression profiles will also reflect this pattern. The differentially expressed proteins were compared between RA and LA to reveal different disease mechanisms underlying AF in the RA and LA. The present study demonstrated that the development of AF in patients with RMVD was associated with significant changes in protein expression in RAA and LAA tissues and that these AF-associated proteins had different distributions in RAA and LAA. Certain AF-associated proteins were differentially expressed both in the RA and LA compared with expression in SR samples, while others were different only in the RA or LA. The current study further demonstrated that the expression of certain proteins were not changed between the RAA and LAA in patients with SR, whereas there is a difference in the protein expression profiles of SR and AF between the RAA and LAA. Therefore, it was hypothesize that differential distribution of these AF-associated proteins may reflect different protein mechanisms in the RA and LA during AF. Genomic (8,17), morphological (18,19), and electrophysiological (20-22) differences have been observed between the RA and LA in mechanisms involved in AF. Thus, the present study provided proteomic evidence that different mechanisms regulate the RA and LA in AF.

Protein expression profiles also reflect certain spatial characteristics (depending on cell, tissue or organ type). The current study observed that the protein expression levels of CRYAB, MSN and transferrin were different when comparing RAA and LAA tissues in patients with RMVD and SR. CRYAB and MSN expression was increased in the

SR-LAA group compared with the SR-RAA group, however they were identified as AF-associated proteins only in RAA tissue. By contrast, transferrin expression was increased in the SR-RAA group compared with the SR-LAA, and was identified as an AF-associated protein only in LAA tissue. These results suggest that CRYAB, MSN and transferrin are tissue dependent AF-associated proteins that may be involved in the progression from SR to AF as observed by the initial expression studies performed in RAA and LAA of RMVD patients with SR. The difference in the initial expression of these proteins between RAA and LAA in patients with RMVD and SR may due to the progress from healthy to RMVD status. Cooley *et al* (36) reported that microRNA expression profiles caused differential changes in the RA and LA with the development from healthy to valvular heart diseased condition. Thus, potentially, the certain proteins become differentially expressed in the RA and LA during RMVD compared with healthy settings. In addition, in patients with RMVD, the association between LA size and AF is well established and LA dilatation is considered to be a cause and a consequence of AF (5). The results of the present study revealed that the LA size of patients with AF was significantly greater than in patients with SR (Table I), thus, potentially, the significant structural remodeling occurring in the LA may also alter the protein expression profiles and cause, at least partially, differential regulation of AF-associated proteins in the RA and LA in patients with RMVD.

The current study identified several AF-associated proteins using 2-D DIGE proteomics analysis. Of these proteins, a number may participate in the mechanisms associated with AF, whereas others maybe a result of AF. The exact role of these differentially expressed proteins in AF requires further investigation. Stringent bioinformatics analysis will be required to select for candidate proteins for future functional studies. Bioinformatics analysis was performed in the current study using the PANTHER and STRING systems to classify AF-associated proteins and predict a protein-protein interaction network (Figs. 5 and 6). This analysis may provide investigators with vital information to direct future research.

A major limitation of this study was the small number of patients. This was due, in part, to the difficulty in finding patients with RMVD and SR. In addition, because the study was performed with human tissues with existing disease, experiments could not be conducted to modulate the protein levels. Therefore, exact targets and pathways by which alterations in these proteins may cause AF in patients with RMVD remain elusive and require further investigation. Finally, patients in this study were a specific cohort with preserved systolic left ventricular function and little comorbidity, undergoing mitral valve replacement surgery. Thus, changes identified in this population may not be representative of other cohort populations.

In conclusion, the current study identified differentially expressed proteins that have potential associations with AF in the RAA and LAA tissues from patients with RMVD. The different distribution of these AF-associated proteins may reflect different mechanisms underlying RAA and LAA involvement in AF. These findings may be useful for the biological understanding of AF in patients with RMVD and suggest potential therapeutic targets for AF.

Acknowledgements

This work is supported by the Pearl River Scholar Program (grant no. 80000-3210003) and the National Natural Science Foundation of China (grant nos. 81370215 and 81500260). The authors wish to acknowledge Dr. Kun-hua Hu (Key Laboratory on Proteomics, Sun Yat-sen University, Guangzhou, China) for his technical expertise. We are grateful to Dr. Gang Dai and Dr. Rong Fang (Key Laboratory on Assisted Circulation, Ministry of Health, Guangzhou, China) for their technical expertise.

References

1. Murphy NF, Simpson CR, Jhund PS, Stewart S, Kirkpatrick M, Chalmers J, MacIntyre K and McMurray JJ: A national survey of the prevalence, incidence, primary care burden and treatment of atrial fibrillation in Scotland. Heart 93: 606-612, 2007.
2. Darby AE and Dimarco JP: Management of atrial fibrillation in patients with structural heart disease. Circulation 125: 945-957, 2012.
3. Rosiak M, Dziuba M, Chudzik M, Cygankiewicz I, Bartczak K, Drozdz J and Wranicz JK: Risk factors for atrial fibrillation: Not always severe heart disease, not always so 'lonely'. Cardiol J 17: 437-442, 2010.
4. Benjamin EJ, Levy D, Vaziri SM, D'Agostino RB, Belanger AJ and Wolf PA: Independent risk factors for atrial fibrillation in a population-based cohort. The Framingham Heart Study. JAMA 271: 840-844, 1994.
5. Carabello BA: Modern management of mitral stenosis. Circulation 112: 432-437, 2005.
6. Nattel S: New ideas about atrial fibrillation 50 years on. Nature 415: 219-226, 2002.
7. Lam L, Lind J and Semsarian C: Application of proteomics in cardiovascular medicine. Int J Cardiol 108: 12-19, 2006.
8. Liu H, Qin H, Chen GX, Liang MY, Rong J, Yao JP and Wu ZK: Comparative expression profiles of microRNA in left and right atrial appendages from patients with rheumatic mitral valve disease exhibiting sinus rhythm or atrial fibrillation. J Transl Med 12: 90, 2014.
9. Deng L, Jia HL, Liu CW, Hu KH, Yin GQ, Ye JW, He CH, Chen JH, Xie YP, Dang R, *et al*: Analysis of differentially expressed proteins involved in hand, foot and mouth disease and normal sera. Clin Microbiol Infect 18: E188-E196, 2012.
10. Lai LP, Lin JL, Lin CS, Yeh HM, Tsay YG, Lee CF, Lee HH, Chang ZF, Hwang JJ, Su MJ, *et al*: Functional genomic study on atrial fibrillation using cDNA microarray and two-dimensional protein electrophoresis techniques and identification of the myosin regulatory light chain isoform reprogramming in atrial fibrillation. J Cardiovasc Electrophysiol 15: 214-223, 2004.
11. De Souza AI, Cardin S, Wait R, Chung YL, Vijayakumar M, Maguy A, Camm AJ and Nattel S: Proteomic and metabolomic analysis of atrial profibrillatory remodelling in congestive heart failure. J Mol Cell Cardiol 49: 851-863, 2010.
12. Modrego J, Maroto L, Tamargo J, Azcona L, Mateos-Cáceres P, Segura A, Moreno-Herrero R, Pérez-Castellanos N, Delpón E, Pérez-Villacastín J, *et al*: Comparative expression of proteins in left and right atrial appendages from patients with mitral valve disease at sinus rhythm and atrial fibrillation. J Cardiovasc Electrophysiol 21: 859-868, 2010.
13. Mayr M, Yusuf S, Weir G, Chung YL, Mayr U, Yin X, Ladroue C, Madhu B, Roberts N, De Souza A, *et al*: Combined metabolomic and proteomic analysis of human atrial fibrillation. J Am Coll Cardiol 51: 585-594, 2008.
14. García A, Eiras S, Parguiña AF, Alonso J, Rosa I, Salgado-Somoza A, Rico TY, Teijeira-Fernández E and González-Juanatey JR: High-resolution two-dimensional gel electrophoresis analysis of atrial tissue proteome reveals down-regulation of fibulin-1 in atrial fibrillation. Int J Cardiol 150: 283-290, 2011.
15. Huang WJ, Zhou R, Zeng XR, Tan XQ, Cheng ZH, Tang MH, Gou LT, Chen LJ, Tong AP, He Y and Yang JL: Comparative proteomic analysis of atrial appendages from rheumatic heart disease patients with sinus rhythm and atrial fibrillation. Mol Med Rep 4: 655-661, 2011.

16. Zhang P, Wang W, Wang X, Wang X, Song Y, Han Y, Zhang J and Zhao H: Protein analysis of atrial fibrosis via label-free proteomics in chronic atrial fibrillation patients with mitral valve disease. PLoS One 8: e60210, 2013.
17. Zhu H, Zhang W, Zhong M, Zhang G and Zhang Y: Differential gene expression during atrial structural remodeling in human left and right atrial appendages in atrial fibrillation. Acta Biochim Biophys Sin (Shanghai) 43: 535-541, 2011.
18. Park JH, Lee JS, Ko YG, Lee SH, Lee BS, Kang SM, Chang BC and Pak HN: Histological and biochemical comparisons between right atrium and left atrium in patients with mitral valvular atrial fibrillation. Korean Circ J 44: 233-242, 2014.
19. Embi AA, Scherlag BJ and Ritchey JW: Glycogen and the propensity for atrial fibrillation: Intrinsic anatomic differences in glycogen in the left and right atria in the goat heart. N Am J Med Sci 6: 510-515, 2014.
20. John B, Stiles MK, Kuklik P, Chandy ST, Young GD, Mackenzie L, Szumowski L, Joseph G, Jose J, Worthley SG, *et al*: Electrical remodelling of the left and right atria due to rheumatic mitral stenosis. Eur Heart J 29: 2234-2243, 2008.
21. Tai CT, Lo LW, Lin YJ and Chen SA: Arrhythmogenic difference between the left and right atria in a canine ventricular pacing-induced heart failure model of atrial fibrillation. Pacing Clin Electrophysiol 35: 188-195, 2012.
22. Li D, Zhang L, Kneller J and Nattel S: Potential ionic mechanism for repolarization differences between canine right and left atrium. Circ Res 88: 1168-1175, 2001.
23. Chen J, Mandapati R, Berenfeld O, Skanes AC, Gray RA and Jalife J: Dynamics of wavelets and their role in atrial fibrillation in the isolated sheep heart. Cardiovasc Res 48: 220-232, 2000.
24. Liu W, Zhou XW, Liu S, Hu K, Wang C, He Q and Li M: Calpain-truncated CRMP-3 and -4 contribute to potassium deprivation-induced apoptosis of cerebellar granule neurons. Proteomics 9: 3712-3728, 2009.
25. Pang J, Liu WP, Liu XP, Li LY, Fang YQ, Sun QP, Liu SJ, Li MT, Su ZL and Gao X: Profiling protein markers associated with lymph node metastasis in prostate cancer by DIGE-based proteomics analysis. J Proteome Res 9: 216-226, 2010.
26. Fu H, Li W, Liu Y, Lao Y, Liu W, Chen C, Yu H, Lee NT, Chang DC, Li P, *et al*: Mitochondrial proteomic analysis and characterization of the intracellular mechanisms of bis(7)-tacrine in protecting against glutamate-induced excitotoxicity in primary cultured neurons. J Proteome Res 6: 2435-2446, 2007.
27. Jin S, Shen JN, Guo QC, Zhou JG, Wang J, Huang G, Zou CY, Yin JQ, Liu SJ, Liu W, *et al*: 2-D DIGE and MALDI-TOF-MS analysis of the serum proteome in human osteosarcoma. Proteomics Clin Appl 1: 272-285, 2007.
28. Tang ZX, Chen GX, Liang MY, Rong J, Yao JP, Yang X and Wu ZK: Selective antegrade cerebral perfusion attenuating the TLR4/NF-kB pathway during deep hypothermia circulatory arrest in a pig model. Cardiology 128: 243-250, 2014.
29. Zrenner B, Ndrepepa G, Karch MR, Schneider MA, Schreieck J, Schömig A and Schmitt C: Electrophysiologic characteristics of paroxysmal and chronic atrial fibrillation in human right atrium. J Am Coll Cardiol 38: 1143-1149, 2001.
30. Huang JL, Lin YJ, Lee PC, Chang HY, Hartono B, Lo LW, Chang SL, Hu YF, Suenari K, Li CH, *et al*: Right atrial substrate remodeling and atrioventricular node conduction properties in patients with paroxysmal atrial fibrillation. Int J Cardiol 158: 447-449, 2012.
31. Casaclang-Verzosa G, Gersh BJ and Tsang TS: Structural and functional remodeling of the left atrium: Clinical and therapeutic implications for atrial fibrillation. J Am Coll Cardiol 51: 1-11, 2008.
32. Matsuyama TA, Tanaka H, Adachi T, Jiang Y, Ishibashi-Ueda H and Takamatsu T: Intrinsic left atrial histoanatomy as the basis for reentrant excitation causing atrial fibrillation/flutter in rats. Heart Rhythm 10: 1342-1348, 2013.
33. Calò L, Lamberti F, Loricchio ML, De Ruvo E, Colivicchi F, Bianconi L, Pandozi C and Santini M: Left atrial ablation versus biatrial ablation for persistent and permanent atrial fibrillation: A prospective and randomized study. J Am Coll Cardiol 47: 2504-2512, 2006.
34. Kim JB, Bang JH, Jung SH, Choo SJ, Chung CH and Lee JW: Left atrial ablation versus biatrial ablation in the surgical treatment of atrial fibrillation. Ann Thorac Surg 92: 1397-1404; discussion 1404-1405, 2011.
35. Jiang Z, Ma N, Yin H, Ding F, Liu H and Mei J: Biatrial ablation versus limited right atrial ablation for atrial fibrillation associated with atrial septal defect in adults. Surg Today 45: 858-863, 2015.
36. Cooley N, Cowley MJ, Lin RC, Marasco S, Wong C, Kaye DM, Dart AM and Woodcock EA: Influence of atrial fibrillation on microRNA expression profiles in left and right atria from patients with valvular heart disease. Physiol Genomics 44: 211-219, 2012.